Increased dopamine D2 receptor activity in the striatum alters the firing pattern of dopamine neurons in the ventral tegmental area

Sabine Krabbe[a,1], Johanna Duda[b], Julia Schiemann[a,2], Christina Poetschke[b], Gaby Schneider[c], Eric R. Kandel[d,e,f,g,h,3], Birgit Liss[b], Jochen Roeper[a,4], and Eleanor H. Simpson[d,e,3,4]

[a]Institute of Neurophysiology, Goethe University, Frankfurt 60590, Germany; [b]Institute of Applied Physiology, University of Ulm, Ulm 89081, Germany; [c]Institute of Mathematics, Goethe University, Frankfurt 60325, Germany; Departments of [d]Psychiatry and [f]Neuroscience, [g]Howard Hughes Medical Institute, and [h]Kavli Institute for Brain Science, Columbia University, New York, NY 10032; and [e]New York State Psychiatric Institute, New York, NY 10032

Contributed by Eric R. Kandel, January 16, 2015 (sent for review December 17, 2014; reviewed by Ann M. Graybiel and Patricio O'Donnell)

There is strong evidence that the core deficits of schizophrenia result from dysfunction of the dopamine (DA) system, but details of this dysfunction remain unclear. We previously reported a model of transgenic mice that selectively and reversibly overexpress DA D2 receptors (D2Rs) in the striatum (D2R-OE mice). D2R-OE mice display deficits in cognition and motivation that are strikingly similar to the deficits in cognition and motivation observed in patients with schizophrenia. Here, we show that in vivo, both the firing rate (tonic activity) and burst firing (phasic activity) of identified midbrain DA neurons are impaired in the ventral tegmental area (VTA), but not in the substantia nigra (SN), of D2R-OE mice. Normalizing striatal D2R activity by switching off the transgene in adulthood recovered the reduction in tonic activity of VTA DA neurons, which is concordant with the rescue in motivation that we previously reported in our model. On the other hand, the reduction in burst activity was not rescued, which may be reflected in the observed persistence of cognitive deficits in D2R-OE mice. We have identified a potential molecular mechanism for the altered activity of DA VTA neurons in D2R-OE mice: a reduction in the expression of distinct NMDA receptor subunits selectively in identified mesolimbic DA VTA, but not nigrostriatal DA SN, neurons. These results suggest that functional deficits relevant for schizophrenia symptoms may involve differential regulation of selective DA pathways.

ventral tegmental area | dopamine D2 receptor | burst activity | NMDA receptor | schizophrenia

Deficits in cognition and motivation are core features of schizophrenia (1, 2). These symptoms are listed in the *Diagnostic and Statistical Manual of Mental Disorders, Fifth Edition* as a diagnostic criterion for schizophrenia spectrum disorder (3) and have a significant impact on patients' overall functioning and quality of life (4, 5). Currently, there are no effective treatments for these disabling aspects of the disease. Therefore, a high priority in the study of schizophrenia is to increase our understanding of the neurobiology of cognitive and motivational deficits. The midbrain dopamine (DA) system affects cognition and motivation in healthy subjects. It includes DA neurons of the ventral tegmental area (VTA), projecting to prefrontal cortex (PFC) and limbic areas (e.g., ventral striatum), and DA neurons of the substantia nigra (SN), projecting to the dorsal striatum (6). Involvement of the midbrain DA system is strongly implicated in both the cognitive and motivational deficits observed in schizophrenia (7, 8). Moreover, it is well documented that the DA system is altered in patients with schizophrenia (reviewed in refs. 9, 10).

To model the increase in striatal DA D2 receptor (D2R) activity observed in patients with schizophrenia, we previously generated transgenic mice that selectively and reversibly overexpress D2Rs in the striatum (D2R-OE mice) (11). In this model, expression of the transgenic D2Rs is restricted to the postsynaptic medium spiny neurons in the striatum and can be temporally regulated. D2R-OE mice display phenotypes strikingly similar to the cognitive and negative symptoms of schizophrenia. Cognitive phenotypes of D2R-OE mice include deficits in working memory tasks, behavioral flexibility, conditional associative learning, and timing (11–14). D2R-OE mice also exhibit phenotypes similar to the negative symptoms of schizophrenia: a deficit in incentive motivation, without disruption of hedonic processes (13, 15–17). We previously reported that these behavioral deficits in striatal D2R-OE mice are accompanied by changes in cortical DA function (11, 18). D2R overexpression restricted to the striatum led to alterations in DA function in the PFC. These alterations include changes in both the amount and rate of turnover of DA in PFC tissue, as well as changes in the activation of D1 receptors in the PFC in vivo. We also identified changes in inhibitory transmission and DA sensitivity in the PFC of D2R-OE mice (18).

The finding that increased D2R expression restricted to the striatum leads to changes in DA function in the cortex suggests that a central component of the DA midbrain system is perturbed in the D2R-OE mice. We therefore set out to determine whether

Significance

Patients with schizophrenia suffer from cognitive and negative deficits that are largely resistant to current therapeutic strategies. Here, using a genetic mouse model that displays phenotypes similar to these cognitive and negative symptoms, we found that increased postsynaptic D2 receptor (D2R) activity in the striatum leads to changes in the firing pattern of presynaptic dopamine (DA) neurons of the midbrain. These alterations occur in the ventral tegmental area (VTA) of the midbrain, but not in the substantia nigra, suggesting that DA pathways may be differently regulated by striatal D2R hyperactivity. The changes in neuron firing patterns were accompanied by a reduction in NMDA receptor subunits selectively in dopaminergic VTA neurons, providing a potential new target for the treatment of schizophrenia symptoms.

Author contributions: S.K., E.R.K., B.L., J.R., and E.H.S. designed research; S.K., J.D., J.S., and C.P. performed research; S.K., J.S., and G.S. analyzed data; and S.K., E.R.K., B.L., J.R., and E.H.S. wrote the paper.

Reviewers: A.M.G., Massachusetts Institute of Technology; and P.O., Pfizer, Inc.

The authors declare no conflict of interest.

[1]Present address: Friedrich Miescher Institute for Biomedical Research, CH-4058 Basel, Switzerland.

[2]Present address: Centre for Integrative Physiology, School of Biomedical Sciences, University of Edinburgh, Edinburgh EH8 9XD, United Kingdom.

[3]To whom correspondence may be addressed. Email: erk5@columbia.edu or es534@columbia.edu.

[4]J.R. and E.H.S. contributed equally to this work.

This article contains supporting information online at www.pnas.org/lookup/suppl/doi:10.1073/pnas.1500450112/-/DCSupplemental.

these changes might be occurring at the level of presynaptic DA neuron activity. To determine if increased postsynaptic D2R activity in the striatum has an impact on the electrophysiological activity of DA midbrain neurons, we performed single-unit extracellular recordings and juxtacellular labeling of individual DA midbrain neurons in vivo from D2R-OE mice and their control littermates. We found that increased D2R activity in the striatum changed the electrophysiological properties of DA neurons in the VTA, whereas DA neurons in the SN remained unaffected. Specifically, we found that in the DA VTA neurons, both the firing frequency and burst activity were reduced in D2R-OE mice compared with controls. When we switched off the transgene in adulthood, the firing frequency was rescued but the decrease in burst activity was not. This dissociation of the two phenotypes may reflect potentially reversible and irreversible components of DA pathophysiology. In vivo burst activity of DA neurons is under powerful control of NMDA receptor currents (19, 20). To investigate a potential molecular mechanism for the observed alterations in the activity of DA neurons, we quantified NMDA receptor subunit mRNA levels in DA neurons of both the mesolimbic and nigrostriatal pathways. Consistent with the electrophysiological deficits, we found a specific reduction of NMDA receptor subunit 1 (NR1) and NR2B expression selectively in mesolimbic DA neurons of the VTA in D2R-OE mice.

Results

Increased D2R Activity in the Striatum Reduces the Firing Rate and Burst Activity of Midbrain DA Neurons Selectively in the VTA, but Not in the SN. To investigate the influence of increased postsynaptic striatal D2R levels on firing patterns of DA midbrain neurons within the basal ganglia network, we carried out single-unit recordings in vivo in isoflurane-anesthetized D2R-OE and littermate control mice. To identify and localize DA neurons unequivocally, we combined extracellular single-unit recordings with juxtacellular single-cell labeling and post hoc immunohistochemistry. The DA cell phenotype was verified by detection of the marker enzyme tyrosine hydroxylase (TH) in neurobiotin-labeled cells. We only included in our data analysis recordings from juxtacellularly labeled and neurochemically identified DA neurons. We focused on DA neurons in the posterior VTA, which project to the PFC or to distinct limbic areas, such as medial regions of the nucleus accumbens (NAc), as well as DA neurons in the SN projecting to the dorsal striatum (21).

Fig. 1 shows representative examples of in vivo activity and identification of DA VTA and DA SN neurons from control and D2R-OE mice. All neurons displayed spontaneous firing rates between 0.1 and 10 Hz, and action potentials occurred regularly or irregularly in a single-spike or bursting pattern. Statistical analysis (Fig. 2 and Table S1) revealed that the mean firing frequencies of DA VTA neurons from D2R-OE mice were about 35% lower compared with the mean firing frequencies of DA VTA neurons from control mice (Fig. 2*A*; control: 3.7 ± 0.4 Hz, $n = 28$ cells, $n = 14$ mice; D2R-OE: 2.4 ± 0.3 Hz, $n = 22$, $n = 8$; t test: $t_{(48)} = 2.7$, $P = 0.010$). The variability of firing for DA VTA neurons [expressed as the coefficient of variation (CV)], however, was not different from D2R-OE mice compared with controls (Table S1). In contrast to the difference in firing frequencies of DA VTA neurons from D2R-OE and control mice, we found no effect of genotype on firing frequencies in DA neurons of the SN (control: 4.6 ± 0.5 Hz, $n = 16$, $n = 8$; D2R-OE: 3.9 ± 0.4 Hz, $n = 14$, $n = 7$; t test: $t_{(28)} = 1.1$, $P = 0.291$).

To analyze burst firing, we initially applied the classical 80/160 ms criterion introduced by Grace and Bunney (22) to identify bursts, which defines an interspike interval of <80 ms as the beginning of a burst and an interval of >160 ms as the ending of a burst. We found that in DA neurons of the VTA from D2R-OE mice, the burst rate was almost fourfold lower compared with controls [Fig. 2*B*; median (25–75% quantiles); control: 4.3 (0.8/16.4) min^{-1}, $n = 28$; D2R-OE: 0.4 (0/4.1) min^{-1}, $n = 22$; Mann–Whitney U (MWU) test: $U_{(28,22)} = 164$, $P = 0.005$]. In addition, the percentage of spikes that were fired within bursts (% SFB) in the DA neurons of the VTA of D2R-OE mice was more than twofold lower compared with controls [Fig. 2*C*; control: 5.3 (1.3/29.6) %, $n = 28$; D2R-OE: 0.5 (0/6.5) %, $n = 22$; MWU test: $U_{(28,22)} = 180.5$, $P = 0.012$]. As with the decreased firing rate in D2R-OE mice, the bursting deficit in D2R-OE mice was specific for DA VTA neurons and not observed in DA SN neurons [Fig. 2*B*; burst rate in control: 2.5 (0.8/14.2) min^{-1}, $n = 16$; burst rate in D2R-OE: 3.6 (0.7/13.8) min^{-1}, $n = 14$; MWU test: $U_{(16,14)} = 103$, $P = 0.868$; and Fig. 2*C*; % SFB in control: 2.7 (0.8/22.3) %, $n = 16$; % SFB in D2R-OE: 5.2 (0.8/21.8) %, $n = 14$; MWU test: $U_{(16,14)} = 107.5$, $P = 0.819$]. We also used the classical 80/160 ms burst criterion to characterize other aspects of burst activity. Thus, we examined intrinsic burst parameters, including mean intraburst frequency, maximum firing frequency, and number of spikes within bursts, but found no differences in these parameters for DA VTA or DA SN neurons between D2R-OE and control mice (Table S1).

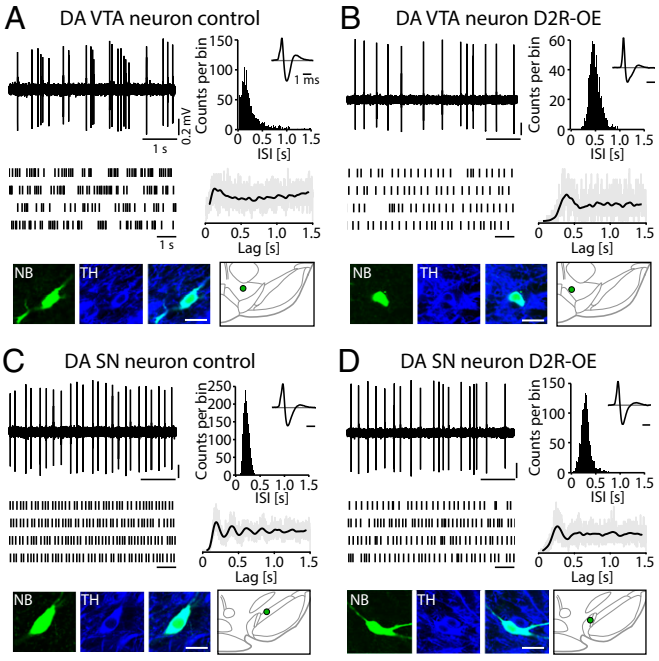

Fig. 1. Electrophysiological in vivo activity of identified DA midbrain neurons in D2R-OE and control mice. (*A*, *Upper*) In vivo single-unit activity of a DA VTA neuron from an isoflurane-anesthetized control mouse (*Left*) and corresponding interspike interval (ISI) histogram (*Right*, >10-min continuous recording). (*Inset*) Triphasic extracellular action potential (averaged waveform). (*A*, *Middle*) Schematic spike train representation of a longer recording period (*Left*) and the autocorrelation histogram (ACH; *Right*) with an initial peak illustrates the bursty activity pattern (>10-min continuous recording; gray lines indicate raw data, and the black line indicates the smoothed ACH fit). (*A*, *Lower*) Confocal images confirm that the neurobiotin (NB)-filled neuron (green) expressed TH (blue) and reveal that it was located in the VTA [green dot; schematic coronal plane relative to bregma −3.6 mm (56)]. (Scale bar: 20 μm.) (*B*) In vivo single-unit recording of a DA VTA neuron from an isoflurane-anesthetized D2R-OE mouse. Data are presented as in *A*. Note the longer ISIs and absence of burst activity in the neuronal activity compared with the DA VTA neuron from a control mouse in *A*. (*C*) In vivo single-unit recording of a DA SN neuron from a control mouse. Data are presented as in *A*. The recurrent equidistant peaks in the ACH reflect the high regularity of the cellular activity. This neuron was located in the rostral SN (coronal plane relative to bregma −3.16 mm). (*D*) In vivo single-unit recording of a DA SN neuron from a D2R-OE mouse. Data are presented as in *A*.

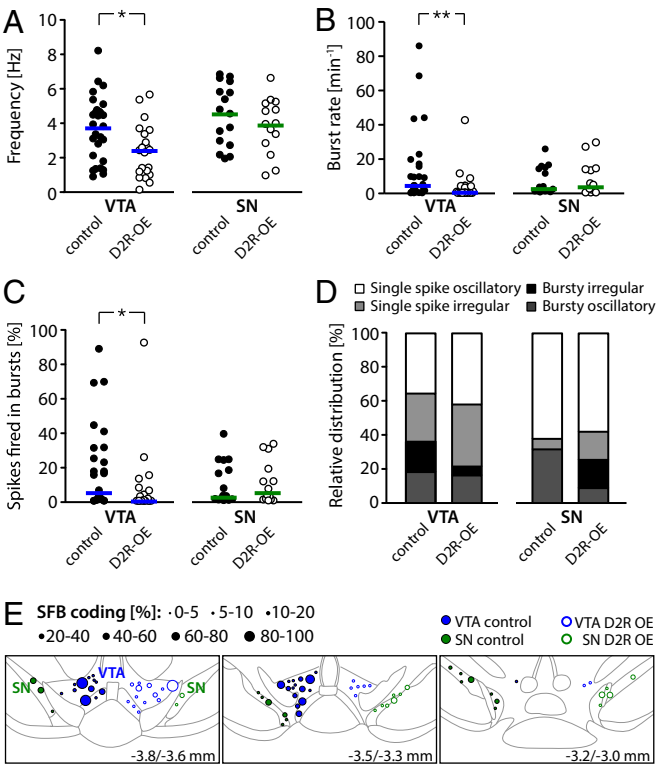

Fig. 2. Analysis of in vivo recordings from DA VTA and DA SN neurons in D2R-OE and control mice. (*A*) Mean firing frequencies of identified DA VTA and DA SN neurons in control and D2R-OE mice; horizontal lines represent the mean. Note the significantly diminished rate in DA VTA neurons from D2R-OE mice compared with controls (DA VTA in control: $n = 28$ cells, $n = 14$ mice; DA VTA in D2R-OE: $n = 22$, $n = 8$; DA SN in control: $n = 16$, $n = 8$, DA SN in D2R-OE: $n = 15$, $n = 7$). (*B*) Mean burst set rate of DA VTA and SN neurons in control and D2R-OE mice; horizontal lines represent the median. Note the significantly diminished rate in DA VTA neurons from D2R-OE mice compared with controls (DA VTA in control: $n = 28$ cells, $n = 14$ mice; DA VTA in D2R-OE: $n = 22$, $n = 8$; DA SN in control: $n = 16$, $n = 8$, DA SN in D2R-OE: $n = 15$, $n = 7$). (*C*) Accordingly, the % SFB was selectively reduced in DA VTA neurons from mice with striatal D2R overexpression. Horizontal lines represent the median (DA VTA in control: $n = 28$ cells, $n = 14$ mice; DA VTA in D2R-OE: $n = 22$, $n = 8$; DA SN in control: $n = 16$, $n = 8$, DA SN in D2R-OE: $n = 15$, $n = 7$). (*D*) Relative distribution of firing patterns in DA VTA and SN neurons defined by GLO-dependent ACH classification (DA VTA in control: $n = 28$, DA VTA in D2R-OE: $n = 19$, DA SN in control: $n = 16$, DA SN in D2R-OE: $n = 12$). (*E*) Functional burst map. DA neurons recorded from control (left side, ●) and D2R-OE (right side, ○) mice are plotted corresponding to their position in the VTA (blue) and SN (green). The symbol size refers to the % SFB. Coronal planes are relative to bregma and are modified from Paxinos and Franklin (56) (also Tables S1–S3). $^*P < 0.05$; $^{**}P < 0.005$.

To analyze firing patterns in a frequency-independent manner, we applied our recently established stochastic model called GLO [Gaussian locking to a free oscillator (23)], which characterizes the main features of global DA spike trains with respect to burstiness and regularity (details are provided in *SI Materials and Methods*). The GLO model classifies spike trains into four patterns: (*i*) single-spike oscillatory, (*ii*) single-spike irregular, (*iii*) bursty oscillatory, and (*iv*) bursty irregular. As evident in Fig. 2*D* and in accordance with the data described above, we observed a decreased percentage of all bursty cells (bursty oscillatory + bursty irregular) in DA VTA neurons (36% in controls, 21% in D2R-OE mice; Table S1). However, we did not find a statistically significant difference between the overall distribution of firing patterns ($P = 0.687$, χ^2 test). Because the GLO model classified DA VTA neurons according to firing pattern, we were able to identify a significant reduction of mean firing rates selectively in single-spike firing DA VTA neurons from D2R-OE mice compared with controls (MWU test: $U_{(18,15)} = 197$, $P = 0.025$). The GLO results suggest that two altered phenotypes are present in DA VTA neurons from D2R-OE mice: frequency reduction and burst rate reduction. We did not find other parameters of the GLO model, such as the degree of regularity of neuronal activity (θ) or the mean number of spikes per burst (λ), to be significantly altered (*SI Materials and Methods* and Tables S2 and S3).

To determine if the reduction in bursting occurred selectively in subregions of the VTA, we generated a map of functional bursting (Fig. 2*E*). This map revealed that most of the recorded DA VTA neurons in WT as well as D2R-OE mice resided in the posterior medial region of the VTA (the paranigral nucleus and the parabrachial pigmented nucleus; Fig. 2*E*, *Upper* and *Middle*). In contrast, our dataset has little coverage in the rostral VTA (Fig. 2*E*, *Lower*). Within the posterior medial VTA, high- and low-bursting VTA DA neurons appeared to be randomly distributed in a "salt and pepper" fashion in control mice. However, in D2R-OE mice, high-bursting VTA neurons appeared to be selectively absent.

Normalizing D2R Activity in the Striatum Rescues the Slow DA VTA Firing Frequency, but Not the Deficit in Burst Activity in D2R-OE Mice. To determine if the lower VTA firing frequency and burst activity observed in D2R-OE mice are due to the chronic or acute overexpression of striatal D2Rs, we switched off the transgene in adulthood in a separate cohort of mice and performed in vivo single-unit recordings on these mice. To switch off the D2R transgene, we fed the mice a doxycycline (Dox)-supplemented chow for 4–5 wk. Fig. 3 shows representative examples of the in vivo activity of DA VTA and DA SN neurons in isoflurane-anesthetized control and D2R-OE mice treated with Dox. The results and statistical analysis are summarized in Fig. 4 and Table S4. Normalization of striatal D2R activity rescued the lower mean firing frequencies in DA VTA neurons in the D2R-OE mice, because there was no longer a difference from the control mice (Fig. 4*A*; control: 4.0 ± 0.6 Hz, $n = 15$, $n = 6$; D2R-OE: 3.7 ± 0.5 Hz, $n = 16$, $n = 6$; t test: $t_{(29)} = 0.4$, $P = 0.713$). In addition, we observed significantly smaller spike train variability (CV) in DA VTA neurons from Dox-treated D2R-OE mice compared with Dox-treated controls (Table S4), suggesting that a greater regularity of firing is associated with increased striatal D2R activity that is limited to the pre- and postnatal development periods. As observed before, DA SN neurons did not show any difference in the mean discharge rates or variability (Fig. 4*A*; control: 4.8 ± 0.6 Hz, $n = 10$, $n = 5$; D2R-OE: 4.4 ± 0.5 Hz, $n = 10$, $n = 4$; t test: $t_{(18)} = 0.6$, $P = 0.569$; Table S4).

In contrast to the normalization of mean firing rates, the burst deficit of DA VTA neurons in D2R-OE mice was not rescued by switching off the transgene. DA VTA neurons still displayed an approximately fourfold reduced burst rate [Fig. 4*B*; control: 4.9 (0.5/53.3) min^{-1}, $n = 15$; D2R-OE: 0.4 (0.03/4.4) min^{-1}, $n = 16$; MWU test: $U_{(15,16)} = 67.5$, $P = 0.039$]. Furthermore, the percentage of spikes occurring in bursts was also persistently and significantly diminished [Fig. 4*C*; control: 5.2 (0.7/53.2) %, $n = 15$; D2R-OE: 0.6 (0.01/4.3) %, $n = 16$; MWU test: $U_{(15,16)} = 65$, $P = 0.031$]. Again, as observed in the non–Dox-treated cohort of mice, there was no effect of genotype on burst activity of DA SN neurons [burst rate of control: 9.7 (2.9/26.1) min^{-1}, $n = 10$; burst rate of D2R-OE: 16.8 (0.6/24.4) min^{-1}, $n = 10$; MWU test: $U_{(10,10)} = 49$, $P = 0.925$; % SFB of control: 9.4 (3.6/41.9) %, $n = 10$; % SFB of D2R-OE: 17.3 (0.5/40.9) %, $n = 10$; WMU test: $U_{(10,10)} = 50.0$, $P = 0.971$]. Again, we detected no difference in intrinsic burst parameters between DA neurons of the VTA or SN in D2R-OE and control mice treated with Dox (Table S4).

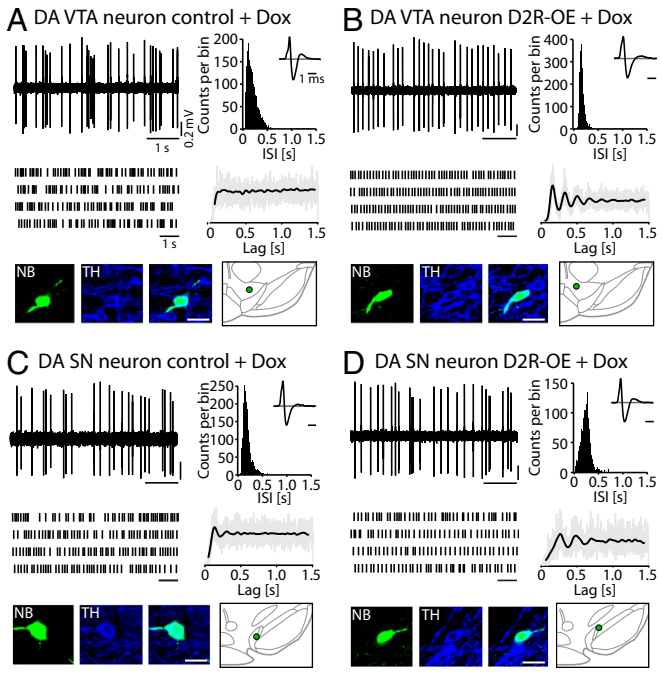

Fig. 3. Electrophysiological in vivo characteristics of identified DA midbrain neurons in D2R-OE and control mice after Dox treatment. (*A*) In vivo single-unit recording of a DA VTA neuron from an isoflurane-anesthetized control mouse after Dox treatment. (*B*) In vivo single-unit recording of a DA VTA neuron from an isoflurane-anesthetized D2R-OE mouse after Dox treatment. Note the similarity of firing frequency and the persistent absence of bursts in the neuronal activity compared with the DA VTA neuron from a control mouse depicted in *A*. (*C*) In vivo single-unit recording of a DA SN neuron from a control mouse after Dox treatment. (*D*) In vivo single-unit recording of a DA SN neuron from a D2R-OE mouse after Dox treatment. All data are presented as in Fig. 1*A*.

As before, the GLO model analysis was concordant with the data described above and showed a persistent trend toward a smaller proportion of burst-firing DA VTA neurons (bursty oscillatory + bursty irregular neurons) recorded from Dox-treated D2R-OE mice compared with Dox-treated controls (25% in controls, 14% in D2R-OE mice; Fig. 4*D* and Table S4). In addition, and consistent with the overall reduction of firing variability in the DA VTA neurons of Dox-treated D2R-OE mice, the relative proportion of regular single-spike firing (i.e., single-spike oscillatory) VTA DA neurons was significantly increased in Dox-treated D2R-OE mice compared with Dox-treated controls (Table S4). Detailed analysis of GLO parameters of single-spike pattern firing DA VTA neurons confirmed their significantly increased regularity [e.g., a decrease in the measure or irregularity, θ, from Dox-treated D2R-OE mice compared with Dox-treated control mice; MWU test: $U_{(9,12)} = 101$, $P = 0.0003$; Tables S2 and S3]. This observed increase in the regularity of activity in single-spike firing DA VTA neurons in Dox-treated D2R-OE mice did not affect the mean firing frequency of these neurons. As reported for all DA VTA subtypes combined, the reduction in mean firing frequency of single-spike firing DA VTA neurons from D2R-OE mice was not evident after Dox treatment (MWU test: $U_{(9,12)} = 52$, $P = 0.92$).

In summary, we identified two altered firing phenotypes in DA VTA neurons from D2R-OE mice: a decrease in mean firing rate that was rescued by switching off the transgene and a reduction in burst firing that persisted after the transgene was switched off.

Increased D2R Activity in the Striatum Reduces the Level of NMDA Receptor Subunit Expression NR1 and NR2B Selectively in Mesolimbic DA VTA, but Not in Nigrostriatal DA SN Neurons. Because reduced bursting emerged as the persistent core deficit in the D2R-OE mice, we focused our molecular analysis on the key player of burst control in DA VTA neurons. Burst activity of the DA cells of the VTA in vivo is under powerful control of NMDA receptors (19, 20). We therefore investigated if the reduction in burst activity observed in the DA VTA neurons of D2R-OE mice might be due to altered NMDA receptor subunit expression in these neurons. To quantify NMDA receptor subunit expression selectively in the DA neurons in identified projection pathways, we combined in vivo retrograde tracing with single-cell laser microdissection (LMD) and quantitative RT-PCR. Fig. 5 depicts representative examples and schematic maps of all injection sites of red fluorescent retrograde tracing beads in either the NAc (core/medial shell region, Fig. 5*A*) or the dorsal striatum (Fig. 5*B*). To obtain strict specificity of mesolimbic and nigrostriatal

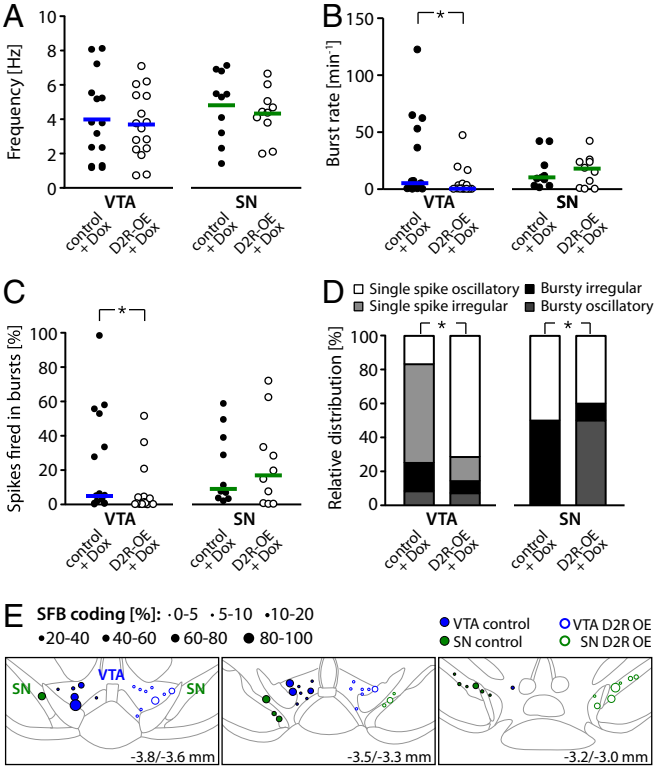

Fig. 4. Analysis of in vivo recordings from DA VTA and SN neurons in D2R-OE and control mice after Dox treatment. (*A*) Mean firing frequencies of identified DA VTA and SN neurons in D2R-OE and control mice after Dox treatment; horizontal lines indicate the mean. Normalization of striatal D2R activity restores the in vivo firing rates of DA VTA neurons in D2R-OE mice to control levels (DA VTA in control: $n = 15$, $n = 6$; DA VTA in D2R-OE: $n = 16$, $n = 6$; DA SN in control: $n = 10$, $n = 5$, DA SN in D2R-OE: $n = 10$, $n = 4$). (*B*) Mean burst rate of DA VTA and SN neurons; horizontal lines represent the median. The burst rate is persistently diminished in DA VTA neurons from D2R-OE mice after 5 wk of Dox treatment (DA VTA in control: $n = 15$, $n = 6$; DA VTA in D2R-OE: $n = 16$, $n = 6$; DA SN in control: $n = 10$, $n = 5$, DA SN in D2R-OE: $n = 10$, $n = 4$). (*C*) % SFB is also persistently reduced in DA VTA neurons after normalization of striatal D2R overexpression. Horizontal lines represent the median (DA VTA in control: $n = 15$, $n = 6$; DA VTA in D2R-OE: $n = 16$, $n = 6$; DA SN in control: $n = 10$, $n = 5$, DA SN in D2R-OE: $n = 10$, $n = 4$). (*D*) Relative distribution of firing patterns in DA VTA and SN neurons defined by GLO-dependent ACH classification after Dox treatment (DA VTA in control: $n = 12$, DA VTA in D2R-OE: $n = 14$, DA SN in control: $n = 8$, DA SN in D2R-OE: $n = 10$). (*E*) Functional burst map. Data are presented as in Fig. 2*E* (also Tables S2–S4). *$P < 0.05$.

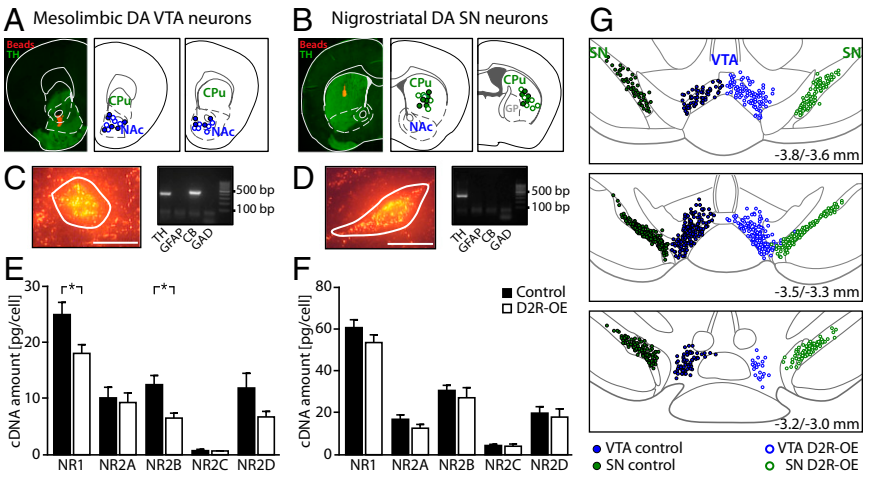

Fig. 5. NMDA receptor subunit mRNA levels in mesolimbic DA VTA and nigrostriatal DA SN neurons of D2R-OE and control mice. (*A*, *C*, and *E*) Mesolimbic DA VTA neurons. (*B*, *D*, and *F*) Nigrostriatal DA SN neurons. (*A*) Mesolimbic DA VTA tracing. (*Left*) Verification of the injection site of red fluorescent retrobeads in the NAc core and shell. TH counterstaining is shown in green. The section is aligned with diagrams from Paxinos and Franklin (56). (*Middle* and *Right*) Schematic mapping of all mesolimbic injection sites [center of injection, coronal planes relative to bregma: 1.70 mm and 1.34 mm; modified from Paxinos and Franklin (56)]. CPu, caudate putamen. (*B*) Nigrostriatal DA SN tracing. Data are presented as in *A*. Injection sites of red fluorescent retrobeads were verified to be in the CPu (coronal planes relative to bregma: 0.86 mm and 0.34 mm). GP, globus pallidus. (*C*) Identification of mesolimbic DA VTA neurons. (*Left*) Single mesolimbic DA VTA neuron in a coronal fixed midbrain section, identified via fluorescent retrobead labeling, before UV-LMD (white line marks cutting line of the laser). (Scale bar: 25 μm.) (*Right*) Agarose gel electrophoresis of UV-LMD multiplex-nested RT-PCR products for positive and negative marker genes. CB, calbindin d-28k, GAD, L-gluatamate decarboxylase 65 and 67. Only TH-positive and GFAP- and GAD-negative cDNA pools from mesolimbic DA neurons were included in the NMDA receptor subunit qPCR expression analysis. (*D*) Identification of nigrostriatal DA SN neurons. Data are presented as in *C*. Only TH-positive and CB-, GFAP-, and GAD-negative cDNA pools from nigrostriatal DA neurons were included in the NMDA receptor subunit qPCR expression analysis. (*E*) RT-qPCR results for NMDA receptor α and β subunits from mesolimbic DA VTA neurons. Note the significantly lower mRNA levels of NR1 and NR2B in D2R-OE mice compared with control mice. Details are provided in Table 1. $*P < 0.05$. (*F*) RT-qPCR results for NMDA receptor subunits from nigrostriatal DA SN neurons. (*G*) Schematic mapping of all neurons dissected by UV-LMD and analyzed by RT-qPCR in the VTA (blue) and SN (green) of control (left side, ●) and D2R-OE (right side, ○) mice. Coronal planes relative to bregma [modified from Paxinos and Franklin (56)].

DA neurons, only cDNA pools (derived from 10 neurons each) that tested positive for the catecholamine neuron marker TH and negative for the astroglial marker GFAP, as well as for the GABAergic neuron markers GAD65 and GAD67, were used for NMDA receptor subunit quantification by quantitative PCR assay. In addition, only calbindin d-28k–negative DA SN cell pools were included in the analysis (21) (Fig. 5 *C* and *D*). We quantified mRNA levels of the NMDA receptor α subunit NR1 and the β subunits NR2A, NR2B, NR2C, and NR2D (Fig. 5*E*). Statistical analysis revealed a significant reduction in mRNA levels for the pore-forming α subunit NR1 and the regulatory β subunit NR2B in mesolimbic DA neurons of the VTA in D2R-OE mice compared with controls (Table 1). In contrast, the expression levels of all NMDA receptor subunits tested were unchanged in nigrostriatal DA SN neurons in D2R-OE mice compared with controls (Fig. 5*F*). A systematic mapping of all DA neurons we analyzed confirmed that collection sites were comparable between D2R-OE and control mice and that these collection sites focused on the posterior medial VTA, as did the electrophysiological experiments (Fig. 5*G* compared with Figs. 2*E* and 4*E*). Table 1 provides a summary of all of the results and statistical analyses of NMDA receptor subunit expression levels in D2R-OE compared with control mice.

In summary, we have found a selective reduction of NMDA receptor NR1 α and NR2B β subunit expression exclusively in mesolimbic DA VTA neurons from D2R-OE mice, consistent with decreased burst firing in DA neurons from the same posterior medial region of the VTA.

Discussion

We have found that an increase in expression of postsynaptic D2Rs in the entire striatum results in selective in vivo changes of the firing patterns of DA neurons in the VTA. This alteration in DA VTA neuron in vivo firing has two main components: (*i*) a decrease in the mean firing frequency of DA VTA neurons and (*ii*) a reduced bursting activity in these neurons. Only one of these components was reversible. Mean firing rates returned to control levels when overexpression of striatal D2Rs was switched off in adult mice with Dox. By contrast, the reduction in burst firing persisted, suggesting that distinct molecular mechanisms are involved in these two components. The fact that the bursting deficit was not reversible implies that there is a critical time window during development during which increased striatal D2R overexpression results in physiological changes that cannot be recovered from. This critical time window likely occurs during prenatal brain development, because we previously found that when D2R-OE transgene expression was restricted to the prenatal period by switching of the transgene from the day of birth, D2R-OE mice showed cognitive deficits in adulthood (11).

In addition to the above phenotypes, switching of the D2R transgene not only reversed the reduction in firing frequency in DA VTA neurons but also generated an additional phenotype in these cells. After Dox treatment, DA VTA neurons showed a significantly increased regularity of the single-spike firing pattern. The emergence of this phenotype only after the transgene was switched off alludes to the complexity and profundity with which increased striatal D2Rs affect the development and functioning of the DA system. The increase in regularity of firing may reflect changes in DA VTA function, resulting from increased postsynaptic striatal D2R activity during pre- and/or postnatal development, that is compensated for, but only while the transgene is active. Several other studies have also demonstrated that genetic or pharmacological perturbations to the DA system during development can result in long-lasting functionally significant changes in different brain regions (e.g. refs. 24–26 and reviewed in ref. 27), suggesting vulnerability that likely has clinical significance.

Table 1. Summary of NMDA receptor subunit expression levels and complete statistical results

NMDAR subunit	Mesolimbic DA VTA neurons						Nigrostriatal DA SN neurons					
	Control	*n*	D2R-OE	*n*	MWU *U* value	*P* value	Control	*n*	D2R-OE	*n*	MWU *U* value	*P* value
NR1	23.0 (17.5–33.1)	29	17.1 (11.8–25.1)	27	253	0.024*	59.2 (50.2–74.3)	30	51.5 (11.7–23.7)	30	358	0.176
NR2A	8.9 (3.8–13.6)	14	7.1 (2.2–13.0)	12	71	0.520	15.0 (11.7–23.7)	15	12.2 (7.5–14.2)	15	72	0.097
NR2B	11.5 (7.9–19.9)	14	6.0 (3.6–9.3)	12	36	0.015*	29.9 (25.2–35.5)	15	24.9 (11.1–39.0)	14	86.5	0.432
NR2C	0.6 (0.4–1.2)	4	0.7 (0.7–1.1)	5	8	0.730	4.7 (2.2–5.6)	10	3.4 (1.4–6.1)	10	39	0.436
NR2D	12.3 (3.6–15.9)	10	5.8 (4.6–9.8)	8	23	0.146	20.1 (12.1–27.2)	10	15.0 (6.3–26.0)	10	43	0.631

Values represent median and (25%/75%) quantiles. MWU tests were used to compare values across genotype. *n*, number of pools of cells used in each test, which were obtained from six animals per genotype. *$P < 0.05$.

Although increased postsynaptic striatal D2R expression and activity were present in the entire striatum in our transgenic model, the observed alterations in the midbrain were DA subtype-selective, affecting neurons that project to the ventral, but not the dorsal, striatum. We found changes in the firing frequency and burst activity of DA neurons of the VTA, but no changes in either parameter in DA neurons in the SN. Therefore, the phenotypes observed were not due to a global effect on midbrain DA neurons.

The finding that increased striatal postsynaptic D2R activity has a selective effect on DA neurons of the VTA, but not the SN, is unexpected, given that both regions of the midbrain receive input (directly or indirectly) from the striatum (28), and suggests that the physiological consequences of striatal postsynaptic D2R hyperactivity are restricted to either a specific output from the striatum and/or a specific input to the midbrain (29). The observation that striatal D2R overexpression selectively disrupted DA VTA neuron activity and spared DA SN neuron activity may not have been predicted based on striatal-midbrain circuitry; however, our findings appear to be fully consistent with the behavioral phenotypes we have observed in D2R-OE mice.

Thus, we previously found a reduction in incentive motivation in D2R-OE mice using two different assays. In one assay, the D2R-OE mice display a reluctance to work for preferred food rewards on a progressive ratio schedule of reinforcement (13, 15). In this task, mice must work increasingly harder to earn successive food rewards, and D2R-OE mice quit after earning fewer rewards than control littermates. In another assay, we found that D2R-OE mice also exert less effort and earn fewer rewards in a current choice paradigm in which the mice can press a lever to obtain a preferred reward (milk) or, instead, consume less preferred food (regular home cage chow) without any work requirement (17). Incentive motivation can be manipulated by modulating DA receptor activity in the NAc (30). Moreover, the level of extracellular DA in the NAc has been found to correlate with the level of motivation during operant schedules of reinforcement (31). Because mean firing frequency of mesolimbic DA VTA neurons regulates the tonic level of extracellular DA in the ventral striatum (32), our findings suggest that the observed deficits in incentive motivation may be a result of the reduction in firing frequency of DA VTA neurons that we report here. Consistent with this idea, both the decreased frequency of DA VTA neuron firing and the deficit in motivation are reversible phenotypes that are rescued by switching the transgene off (13, 17). The transient reduction in mean firing rates could be due to changes in intrinsic pacemaker properties of DA VTA neurons and/or the result of an altered afferent drive; these possibilities remain to be elucidated. However, the concomitant higher regularity of spike trains in D2R-OE mice after Dox treatment may be an indication that intrinsic pacemaker properties, particularly small conductance calcium-activated potassium channels (33) in DA VTA neurons, may be affected by changes in striatal D2R activity. In contrast, alterations in synaptic excitation/inhibition balance ($GABA_A$ receptors/AMPA receptors) would primarily affect burst rate and burst length (34).

In addition to displaying motivation deficits, D2R-OE mice show significant deficits in both learning and performing distinct types of cognitive tasks. Specifically, D2R-OE mice show deficits in several behavioral assays involving cue-dependent learning, specifically a "delayed-non-match-to-sample" t-maze task (11), a temporal discrimination task (13), and a conditional associative learning task (12). Such cue-dependent learning is thought to involve the phasic activity in mesolimbic DA VTA neurons. The relationship between DA VTA neuron burst firing and the presentation of cues that predict rewards has been observed to change systematically as animals learn the attributes of the cue-reward relationship (35, 36). A causal role for DA VTA neuron burst activity in cue-dependent learning has also been suggested by the finding that genetic disruption of burst activity resulted in altered cue-dependent learning (20), as well as by recent evidence from optogenetic studies (37). It therefore seems most likely that the reduction in DA VTA neuron burst activity presented here may underlie the deficits in cue-dependent learning that we previously reported in the D2R-OE mice. This idea is supported by the observation that both the reduction in burst firing and cue-dependent learning deficits persist after the transgene is switched off.

The fact that burst activity in the VTA was not rescued after switching off the D2R transgene suggests that this physiological phenotype may be due to the perturbation of a developmental process caused by increased striatal D2R activity during pre- and/or postnatal maturation. Such persistent developmental changes often occur at the level of gene transcription (e.g., refs. 38, 39). We therefore wondered whether the persistent reduction in burst activity in DA VTA neurons of the D2R-OE mice may be due to altered NMDA receptor expression. Indeed, it has previously been found that tonic activation of NMDA receptors causes spontaneous burst activity in DA VTA neurons in vivo (19). In addition, genetic inactivation of NMDA receptor function in DA VTA neurons has been found to disrupt not only in vivo burst firing but also cue-dependent learning (20, 40). To quantify NMDA receptor subunit expression in DA neurons from the VTA and the SN in a segregated way, we combined in vivo retrograde tracing of mesolimbic and mesostriatal DA neurons with UV-LMD of individual fluorescently labeled neurons and RT-quantitative PCR. This approach allowed us to isolate a particular projection pathway selectively within the mesocorticolimbic DA system located in the VTA (21). We chose to isolate the mesolimbic projection to the NAc (core/medial shell) because burst activity in this pathway is known to play a role in cue-dependent learning (30), which is disrupted in D2R-OE mice (11, 12). We found a reduction in the expression levels of NMDA receptor subunits NR1 and NR2B in mesolimbic DA VTA neurons from D2R-OE mice, which may be sufficient to cause the reduction in burst firing that we observed in these cells (20, 40). In contrast, we did not observe any

changes in NMDA receptor expression in nigrostriatal DA SN cells, which project to dorsal parts of the striatum. This finding supports the idea that selective down-regulation of these receptor subunits in DA VTA neurons in D2R-OE mice is responsible for the reduction in burst firing observed selectively in these cells.

How striatal D2R overexpression drives a specific reduction in VTA NMDA receptors is intriguing, particularly because both VTA and SN receive inputs from the striatum (28). It may be that DA VTA neurons are more sensitive to the increased D2R signaling from the striatum compared with DA SN neurons and that the down-regulation in NMDA receptors is a response to regulate the balance of activity in the mesolimbic circuit. A dysfunction of NR2B-containing NMDA receptors is likely to be particularly relevant during prenatal and early postnatal development, when these receptors are the dominant receptor species in DA VTA neurons (41). Subsequently, early postnatal synaptic maturation leads to a switch to predominantly NR2A-containing receptors. In contrast, DA SN neurons are lacking such a subunit switch, and thus this critical window during development. DA SN neurons exhibit NMDA receptors with a different subunit composition throughout their lifetime (42, 43). Additional experiments are required to understand the differential impact on DA VTA and SN neurons. For example, it would be informative to know if NMDA receptors would be down-regulated if D2R-OE expression were restricted to prenatal development. Also, a restriction of the overexpression only to the ventral striatal neurons that project to the VTA could offer valuable clues as to whether this projection is responsible for the observed deficits or if the mechanism involves broader circuitry.

The behavioral processes that are disrupted in D2R-OE mice have been found to be affected by perturbations in the mesocorticolimbic DA system (30). Behavioral pharmacological studies have found that within the mesocorticolimbic system, deficits in either the mesolimbic or mesocortical pathway could underlie deficits similar to the ones observed in D2R-OE mice (30). Unlike in our molecular study, we could not distinguish between mesocortical and mesolimbic DA VTA neurons in our in vivo recordings, and therefore we cannot conclude whether one or both populations of neurons are affected. However, our in vivo recording approach was not likely to bias which of these two similar subtypes of neurons within the VTA we examined. In addition, mean firing rates and burstiness were reduced over the whole extent of the VTA area that we assayed (Fig. 2*E*), which particularly focused on the posterior medial VTA, where both mesolimbic and mesocortical neurons are located (21, 44). Thus, it is likely that the deficits in firing rates and burst activity occur in both mesolimbic and mesocortical neurons.

In contrast to our findings in the VTA, we found that DA SN neurons projecting to the dorsal parts of the striatum were not affected in either their in vivo activity or NMDA receptor subunit expression level. These findings are consistent with the absence of gross motor deficits in D2R-OE mice (11). The finding of a decrease in activity in VTA, and not SN, DA projection neurons also seems to be consistent with recent findings in patients with schizophrenia. Using PET imaging, Slifstein et al. (45) have measured a decrease in DA release in cortical and other extrastriatal regions in patients compared with healthy controls. This widespread blunting of DA release is in contrast to the increase in DA release found selectively in the associative striatum that has been well documented in patients with schizophrenia (10, 46). Like the dorsal striatum in mice, the associative striatum in humans receives its DA input from the SN. Therefore, one potential explanation for the bidirectional changes in DA release observed in the associative striatum vs. extrastriatal regions in patients may be differential changes in the VTA vs. SN subregions of the midbrain. Our D2R-OE mouse model suggests that alterations in postsynaptic D2R activity can result in such differential changes.

In summary, our findings demonstrate that the firing patterns of DA neurons in the VTA are selectively altered in vivo in mice with increased postsynaptic striatal D2R activity, a phenotype we created to model the increase in striatal D2R occupancy observed in patients with schizophrenia (46). This altered firing pattern may be the result of a down-regulation of the NMDA receptor subunits NR1 and NR2B exclusively in this neuronal population at the level of transcription. Although the electrophysiological properties of identified DA neurons cannot be routinely studied in humans, there are data from patients that are consistent with our findings. Patients with schizophrenia show reduced activation of the midbrain in response to reward stimuli compared with healthy control subjects (47). Such blunted activation is associated with reduced functional connectivity between the midbrain and cortical regions during reward processing in patients with schizophrenia (48).

The data that we present here may explain some of the earlier descriptive data that we previously published on the D2R-OE mice. We found that D2R overexpression in the striatum has an impact on DA levels, rates of DA turnover, and activation of D1 receptors in the PFC (11), and we suggested that these changes in cortical DA may underlie the deficits we observed in cortical-dependent cognitive tasks in D2R-OE mice. Here, we show that burst firing is reduced in DA neurons in an area of the midbrain that includes cells projecting to the PFC. Therefore, this model demonstrates the possibility that changes in striatal DA signaling that are similar to changes in striatal DA signaling observed in patients with schizophrenia may result in cognitive cortical deficits via changes in the physiological properties of midbrain DA neurons.

To our knowledge, there are no studies to date addressing NMDA receptor expression levels in identified DA midbrain neurons of patients with schizophrenia, although decreases in NMDA receptor subunit mRNA have been found in the cortex (49–51). Therefore, it now becomes of interest to look at the NMDA receptor protein or mRNA levels in postmortem midbrain tissue from patients with schizophrenia. If molecular changes occur in patients similar to those molecular changes observed in our mouse model, selective pharmacological modulation of NMDA receptor activity might provide a potential target for treatment of the cognitive deficits in schizophrenia, for which there are currently no efficacious therapeutic strategies available.

Materials and Methods

Animals. All procedures were carried out according to the guidelines of the German Tierschutzgesetz and were approved by the Regierungspräsidium Darmstadt (V54-19c 20/15-F40/29) and Regierungspräsidium Tübingen (Aktenzeichen 35/9185.81-3; TV-No. 1043). D2R-OE mice were generated and bred at Columbia University, as described previously. More details are provided in *SI Materials and Methods*. All experiments were performed on male adult D2R-OE mice paired with control littermates (age range of pairs was 3–10 mo). Temporal regulation of transgene expression was achieved by feeding adult mice with Dox-supplemented chow (40 mg/kg; Bio-Serv) for 4–5 wk.

In Vivo Extracellular Single-Unit Recordings and Juxtacellular Labeling. In vivo extracellular single-unit recordings and juxtacellular labeling were essentially as described previously (52). In brief, single units of DA VTA and DA SN neurons were extracellularly recorded in isoflurane-anesthetized mice. After recording (≥10 min), neurons were selectively labeled with neurobiotin using the juxtacellular technique (53) and subjected to immunohistochemical analysis for verification of the DA phenotype and localization within the midbrain subnuclei. Only identified DA neurons (TH-positive cells) were included in the analysis. Details of in vivo extracellular single-unit recordings as well as immunohistochemistry and confocal analysis are provided in *SI Materials and Methods*.

Retrograde Tracing. Retrograde tracing was essentially as described previously (21). Rhodamine-coupled latex microspheres (Retrobeads; Lumafluor) were

injected bilaterally into the ventral striatum (specifically the core and medial shell region of the NAc) or unilaterally into the dorsal striatum of D2R-OE and littermate control mice. Experimental details are provided in *SI Materials and Methods*.

UV-LMD and Quantitative Real-Time PCR of Retrogradely Labeled Neurons. UV-LMD and RT of mRNA from retrobead-labeled neurons, as well as multiplex-nested PCR and quantitative real-time PCR (qPCR), were performed essentially as previously described (54, 55). The mRNA values are given with respect to a relative cDNA standard, derived from mouse midbrain tissue. Details of data analysis, TaqMan primers, probes, and standard curve details for RT-qPCR quantification of NMDA receptor subunits are provided in *SI Materials and Methods* and Table S5.

Statistical Analyses.

Electrophysiology experiments. Datasets were analyzed for Gaussian distribution using the Kolmogorov–Smirnov test. When the null hypothesis of normal distribution was not rejected, the data from each genotype were statistically compared by a Student's *t* test, and the data values are expressed as means ± SEM. When the null hypothesis of normal distribution was rejected, the data from each genotype were statistically compared using a MWU test, and we provide median values and 25–75% quantiles. The distribution of in vivo firing patterns was analyzed using Pearson's χ^2 test. In case of a significant result, individual tests were carried out using Fisher's exact test for each pattern class by pooling the other three groups. Resulting *P* values were compared with Bonferroni-corrected α-level values. For all electrophysiological analysis, "*n*" indicates the number of analyzed neurons and "*N*" indicates the number of animals from which these neurons were derived, which was always $N \geq 4$ animals per group.

Gene expression experiments. All expression data were analyzed using a MWU test, and we present median values and 25–75% quantiles. For expression analysis, *n* indicates the number of neuronal pools analyzed. The number of animals, indicated by *N*, from which these neuronal pools were derived is provided in *Results* and was always $N = 6$ animals per group.

In all figures and tables, statistical significance levels were indicated as $P < 0.05$ (*), $P < 0.01$ (**), or $P < 0.001$ (***). All statistical analyses were carried out with Prism 5 (GraphPad Software), SPSS 19 (IBM Corporation), Microsoft Excel (Microsoft Corporation), MATLAB (R2013b; Mathworks), or R (www.r-project.org).

ACKNOWLEDGMENTS. We thank Silvi Hoidis, Anna-Maria Kashiotis, Annika Parg, Harald Schalk, Stefanie Schulz, and Desiree Spaich for excellent technical assistance; Pete Magill for sharing his protocol for juxtacellular labeling of DA neurons in vivo and Raphaela Bauer for teaching S.K. this method; Jan Gründemann for providing Igor Pro codes and MATLAB analyses; and Iram Haq for maintaining and genotyping the transgenic mouse colony. This work was supported by NIH Grant MH086404 (to E.H.S. and E.R.K.), the Howard Hughes Medical Institute (E.R.K.), Deutsche Forschungsgemeinschaft (DFG) Grant SFB1080 (to J.R.), DFG Grant SPP1665 (to G.S. and J.R.), DFG Grant SFB497, DFG Grant Li 1745/1 (to B.L.), Austrian Science Fund Grant SFB F4412 (to B.L.), the Alfried Krupp Prize (to B.L.), and a Bundesministerium für Bildung und Forschung grant from Nationalen Genomforschungsnetz (01GS08134) (to B.L. and J.R.).

1. Bleuler E (1950) *Dementia Praecox or the Group of Schizophrenias* (International Universities Press, New York), trans Zinkin J.
2. Kraepelin E (1919) *Dementia Praecox and Paraphrenia* (Kreiger Publishing Company, Huntington, NY), trans Barclay RM.
3. APA (2013) *Diagnostic and Statistical Manual of Mental Disorders* (American Psychiatric Publishing, Arlington, VA), 5th Ed.
4. Barch DM (2005) The cognitive neuroscience of schizophrenia. *Annu Rev Clin Psychol* 1:321–353.
5. Rabinowitz J, et al. (2012) Negative symptoms have greater impact on functioning than positive symptoms in schizophrenia: Analysis of CATIE data. *Schizophr Res* 137(1-3):147–150.
6. Roeper J (2013) Dissecting the diversity of midbrain dopamine neurons. *Trends Neurosci* 36(6):336–342.
7. Cools R, D'Esposito M (2011) Inverted-U-shaped dopamine actions on human working memory and cognitive control. *Biol Psychiatry* 69(12):e113–e125.
8. Da Cunha C, Gomez-A A, Blaha CD (2012) The role of the basal ganglia in motivated behavior. *Rev Neurosci* 23(5-6):747–767.
9. Howes OD, et al. (2012) The nature of dopamine dysfunction in schizophrenia and what this means for treatment. *Arch Gen Psychiatry* 69(8):776–786.
10. Kuepper R, Skinbjerg M, Abi-Dargham A (2012) The dopamine dysfunction in schizophrenia revisited: New insights into topography and course. *Handbook Exp Pharmacol* (212):1–26.
11. Kellendonk C, et al. (2006) Transient and selective overexpression of dopamine D2 receptors in the striatum causes persistent abnormalities in prefrontal cortex functioning. *Neuron* 49(4):603–615.
12. Bach ME, et al. (2008) Transient and selective overexpression of D2 receptors in the striatum causes persistent deficits in conditional associative learning. *Proc Natl Acad Sci USA* 105(41):16027–16032.
13. Drew MR, et al. (2007) Transient overexpression of striatal D2 receptors impairs operant motivation and interval timing. *J Neurosci* 27(29):7731–7739.
14. Ward RD, et al. (2009) Impaired timing precision produced by striatal D2 receptor overexpression is mediated by cognitive and motivational deficits. *Behav Neurosci* 123(4):720–730.
15. Simpson EH, et al. (2011) Pharmacologic rescue of motivational deficit in an animal model of the negative symptoms of schizophrenia. *Biol Psychiatry* 69(10):928–935.
16. Ward RD, Simpson EH, Kandel ER, Balsam PD (2011) Modeling motivational deficits in mouse models of schizophrenia: Behavior analysis as a guide for neuroscience. *Behav Processes* 87(1):149–156.
17. Ward RD, et al. (2012) Dissociation of hedonic reaction to reward and incentive motivation in an animal model of the negative symptoms of schizophrenia. *Neuropsychopharmacology* 37(7):1699–1707.
18. Li YC, Kellendonk C, Simpson EH, Kandel ER, Gao WJ (2011) D2 receptor overexpression in the striatum leads to a deficit in inhibitory transmission and dopamine sensitivity in mouse prefrontal cortex. *Proc Natl Acad Sci USA* 108(29):12107–12112.
19. Chergui K, et al. (1993) Tonic activation of NMDA receptors causes spontaneous burst discharge of rat midbrain dopamine neurons in vivo. *Eur J Neurosci* 5(2):137–144.
20. Zweifel LS, et al. (2009) Disruption of NMDAR-dependent burst firing by dopamine neurons provides selective assessment of phasic dopamine-dependent behavior. *Proc Natl Acad Sci USA* 106(18):7281–7288.
21. Lammel S, et al. (2008) Unique properties of mesoprefrontal neurons within a dual mesocorticolimbic dopamine system. *Neuron* 57(5):760–773.
22. Grace AA, Bunney BS (1984) The control of firing pattern in nigral dopamine neurons: burst firing. *J Neurosci* 4(11):2877–2890.
23. Bingmer M, Schiemann J, Roeper J, Schneider G (2011) Measuring burstiness and regularity in oscillatory spike trains. *J Neurosci Methods* 201(2):426–437.
24. Brami-Cherrier K, et al. (2014) Epigenetic reprogramming of cortical neurons through alteration of dopaminergic circuits. *Mol Psychiatry* 19(11):1193–1200.
25. Jones LB, et al. (2000) In utero cocaine-induced dysfunction of dopamine D1 receptor signaling and abnormal differentiation of cerebral cortical neurons. *J Neurosci* 20(12):4606–4614.
26. Levine MS, et al. (1996) Modulatory actions of dopamine on NMDA receptor-mediated responses are reduced in D1A-deficient mutant mice. *J Neurosci* 16(18):5870–5882.
27. Money KM, Stanwood GD (2013) Developmental origins of brain disorders: Roles for dopamine. *Front Cell Neurosci* 7:260.
28. Haber SN, Knutson B (2010) The reward circuit: Linking primate anatomy and human imaging. *Neuropsychopharmacology* 35(1):4–26.
29. Watabe-Uchida M, Zhu L, Ogawa SK, Vamanrao A, Uchida N (2012) Whole-brain mapping of direct inputs to midbrain dopamine neurons. *Neuron* 74(5):858–873.
30. Salamone JD, Correa M (2012) The mysterious motivational functions of mesolimbic dopamine. *Neuron* 76(3):470–485.
31. Ostlund SB, Wassum KM, Murphy NP, Balleine BW, Maidment NT (2011) Extracellular dopamine levels in striatal subregions track shifts in motivation and response cost during instrumental conditioning. *J Neurosci* 31(1):200–207.
32. Floresco SB, West AR, Ash B, Moore H, Grace AA (2003) Afferent modulation of dopamine neuron firing differentially regulates tonic and phasic dopamine transmission. *Nat Neurosci* 6(9):968–973.
33. Soden ME, et al. (2013) Disruption of dopamine neuron activity pattern regulation through selective expression of a human KCNN3 mutation. *Neuron* 80(4):997–1009.
34. Henny P, et al. (2012) Structural correlates of heterogeneous in vivo activity of midbrain dopaminergic neurons. *Nat Neurosci* 15(4):613–619.
35. Schultz W, Dayan P, Montague PR (1997) A neural substrate of prediction and reward. *Science* 275(5306):1593–1599.
36. Hollerman JR, Schultz W (1998) Dopamine neurons report an error in the temporal prediction of reward during learning. *Nat Neurosci* 1(4):304–309.
37. Steinberg EE, et al. (2013) A causal link between prediction errors, dopamine neurons and learning. *Nat Neurosci* 16(7):966–973.
38. Hummler E, et al. (1994) Targeted mutation of the CREB gene: Compensation within the CREB/ATF family of transcription factors. *Proc Natl Acad Sci USA* 91(12):5647–5651.
39. Iacobas DA, Iacobas S, Urban-Maldonado M, Spray DC (2005) Sensitivity of the brain transcriptome to connexin ablation. *Biochim Biophys Acta* 1711(2):183–196.
40. Wang LP, et al. (2011) NMDA receptors in dopaminergic neurons are crucial for habit learning. *Neuron* 72(6):1055–1066.
41. Bellone C, Mameli M, Lüscher C (2011) In utero exposure to cocaine delays postnatal synaptic maturation of glutamatergic transmission in the VTA. *Nat Neurosci* 14(11):1439–1446.
42. Brothwell SL, et al. (2008) NR2B- and NR2D-containing synaptic NMDA receptors in developing rat substantia nigra pars compacta dopaminergic neurones. *J Physiol* 586(3):739–750.
43. Lammel S, Ion DI, Roeper J, Malenka RC (2011) Projection-specific modulation of dopamine neuron synapses by aversive and rewarding stimuli. *Neuron* 70(5):855–862.
44. Ikemoto S (2007) Dopamine reward circuitry: Two projection systems from the ventral midbrain to the nucleus accumbens-olfactory tubercle complex. *Brain Res Brain Res Rev* 56(1):27–78.
45. Slifstein M, et al. (2015) Deficits in prefrontal cortical and extrastriatal dopamine release in schizophrenia: A positron emission tomographic functional magnetic resonance imaging study. *JAMA Psychiatry*, 10.1001/jamapsychiatry.2014.2414.

46. Abi-Dargham A, et al. (2000) Increased baseline occupancy of D2 receptors by dopamine in schizophrenia. *Proc Natl Acad Sci USA* 97(14):8104–8109.
47. Murray GK, et al. (2008) Substantia nigra/ventral tegmental reward prediction error disruption in psychosis. *Mol Psychiatry* 13(3):239, 267–276.
48. Gradin VB, et al. (2013) Salience network-midbrain dysconnectivity and blunted reward signals in schizophrenia. *Psychiatry Res* 211(2):104–111.
49. Beneyto M, Meador-Woodruff JH (2008) Lamina-specific abnormalities of NMDA receptor-associated postsynaptic protein transcripts in the prefrontal cortex in schizophrenia and bipolar disorder. *Neuropsychopharmacology* 33(9):2175–2186.
50. Sokolov BP (1998) Expression of NMDAR1, GluR1, GluR7, and KA1 glutamate receptor mRNAs is decreased in frontal cortex of "neuroleptic-free" schizophrenics: Evidence on reversible up-regulation by typical neuroleptics. *J Neurochem* 71(6):2454–2464.
51. Weickert CS, et al. (2013) Molecular evidence of N-methyl-D-aspartate receptor hypofunction in schizophrenia. *Mol Psychiatry* 18(11):1185–1192.
52. Schiemann J, et al. (2012) K-ATP channels in dopamine substantia nigra neurons control bursting and novelty-induced exploration. *Nat Neurosci* 15(9):1272–1280.
53. Pinault D (1996) A novel single-cell staining procedure performed in vivo under electrophysiological control: Morpho-functional features of juxtacellularly labeled thalamic cells and other central neurons with biocytin or Neurobiotin. *J Neurosci Methods* 65(2):113–136.
54. Dragicevic E, et al. (2014) Cav1.3 channels control D2-autoreceptor responses via NCS-1 in substantia nigra dopamine neurons. *Brain* 137(Pt 8):2287–2302.
55. Schlaudraff F, et al. (2014) Orchestrated increase of dopamine and PARK mRNAs but not miR-133b in dopamine neurons in Parkinson's disease. *Neurobiol Aging* 35(10): 2302–2315.
56. Paxinos G, Franklin KBJ (2007) *The Mouse Brain in Stereotaxic Coordinates* (Academic, New York).